Talanta 120 (2014) 262–267

Contents lists available at ScienceDirect

Talanta

journal homepage: www.elsevier.com/locate/talanta

Preventing UV induced cell damage by scavenging reactive oxygen species with enzyme-mimic Au–Pt nanocomposites

Bin Xiong [1], Ruili Xu [1], Rui Zhou, Yan He *, Edward S. Yeung

State Key Laboratory of Chemo/Biosensing and Chemometrics, College of Chemistry and Chemical Engineering, College of Biology Hunan University, Changsha 410082, China

ARTICLE INFO

Article history:
Received 10 October 2013
Received in revised form
3 December 2013
Accepted 5 December 2013
Available online 14 December 2013

Keywords:
Enzyme-mimic nanomaterials
Reactive active species
Ultraviolet irradiation
Cell imaging

ABSTRACT

We have prepared enzyme-mimic Au–Pt nanocomposites (NCs) for catalyzing the decomposition of reactive oxygen species. After surface modification, the Au–Pt NCs can be readily internalized and retained by human skin cells and also can effectively reduce cellular oxidative stress. We have demonstrated that the active and biocompatible Au–Pt nanocomposites can be applied for preventing cell damages by scavenging cellular reactive oxygen species induced by ultraviolet irradiation, indicating potential uses for the prevention and therapy of ROS-mediated diseases.

© 2013 Elsevier B.V. All rights reserved.

1. Introduction

Due to the increasing crisis in air pollution and depletion of the ozone layer in recent years, ultraviolet (UV) irradiation caused damage has become an important issue in biomedical research [1,2]. One of the major pathways of UV induced cell damage is by producing excessive reactive oxygen species (ROS) such as superoxide anion radical, singlet oxygen, hydrogen peroxide and hydroxyl radical, which could result in cellular injuries including damage of membrane lipid, cellular proteins and nucleic acids [3,4]. Previous reports indicate that intracellular endogenous enzymes including superoxide dismutase (SOD) and catalase may be insufficient to protect cells from sudden oxidative stress such as UV irradiation or drug stimulation [5–7]. This problem can be partially solved by using nanomaterials (NMs) with high catalytic activity to scavenge cellular ROS. Several types of nanomaterials such as nano-Pt, nano-CeO_2, nano-Fe_2O_3, and fullerenes, have been shown to perform like antioxidative enzymes to clear ROS in cancer cells [8–11]. While these studies demonstrated the potential applicability of active NMs against cellular oxidative stress, it is much more interesting to prevent sudden oxidative damage to non-malignant cells caused by UV light or drugs. Intuitively, protecting cells from ROS induced oxidative damage is both dependent on the activity of the NMs for ROS clearance and the amount of NMs internalized and retained by cells. However, many types of nanoparticles are readily uptaken by malignant cells but not so easily by normal cells [12]. Thus, it is crucial to develop nanoparticles with both high ROS-scavenging activity and cellular uptake efficiency.

In the past, several groups have reported that various Pt nanoparticles and Au–Pt NMs exhibit high catalytic activity for clearing superoxides and peroxides *in vitro* [13–16]. However, their ability in ROS clearance in living cells has not been investigated. Herein, we prepared enzyme-mimic Au–Pt nanocomposites (NCs) for scavenging intracellular ROS and protecting against UV induced damage in human skin cell. The surface functionalized Au–Pt NCs can be readily internalized by these non-cancer cells with quite high efficiency, and display excellent biocompatibility and capability to reduce cellular oxidative stress *in vivo*. With the protection of the active Au–Pt NCs, the cellular ROS stress due to UV irradiation was markedly reduced and the subsequent oxidative damages such as alterations in cell morphology and cell proliferation were also effectively diminished. The demonstration of protection from UV induced oxidative damage by scavenging intracellular ROS with active Au–Pt NCs provides interesting alternatives in biomedicine for the prevention and therapy of oxidative stress related diseases.

2. Material and methods

2.1. Chemicals

The chemicals including $NaBH_4$, $C_{19}H_{42}NBr$ (CTAB), $HAuCl_4$, $AgNO_3$, ascorbic acid, H_2PtCl_6, NaH_2PO_4, Na_2HPO_4, H_2O_2, methionine, EDTA,

* Corresponding author.
E-mail address: yanhe2021@gmail.com (Y. He).
[1] These authors contributed equally to this work.

0039-9140/$ - see front matter © 2013 Elsevier B.V. All rights reserved.
http://dx.doi.org/10.1016/j.talanta.2013.12.020

riboflavin, DMSO, bovine serum albumin (BSA) were AR grade and purchased from Shanghai Sinopharm. The carboxy-H2DCFDA was purchased from Invitrogen. Other chemicals including (11-mercaptoundecyl)-N,N,N-trimethylammonium bromide (MUTAB), nitro-blue-tetrazolium chloride (NBT), superoxide dismutase (SOD) and catalase were obtained from Sigma-Aldrich.

2.2. Preparation and characterization of materials

The synthesis processes of gold nanorods (GNRs) were described in our previous work [17]. The GNRs with a LSPR peak at 650 nm were centrifuged twice for removing the residual reagents and then used as seeds for the growth of Au–Pt NCs according to previous reports with some modifications [18]. Typically, 58 μL of 0.0193 M H_2PtCl_6 was added into 9 mL of the synthesized AuNRs under stirring. Then 112 μL of 0.1 M ascorbic acid solution was added into the mixture. After a continuous stirring for 2 min, the solution was transferred into water bath and kept still at 30° over night. The excessive surfactants in the solution were removed by centrifugation and the Au–Pt NCs were redispersed in water by ultrasonication. The purified Au–Pt NCs were characterized with UV–visible spectroscopy (Shimadzu UV-1800, Japan) and transmission electron microscopy (TEM) equipped with an energy-dispersive X-ray (EDX) spectrometer (JEM 3100F, JEOL, Japan). The small Pt nanoparticles were prepared by using $NaBH_4$ as reducing agent according to previous reports [19].

2.3. Determining the ROS-scavenging activity of Au–Pt NCs

2.3.1. Superoxides scavenging by nitro-blue-tetrazolium reduction assays

Because the colorless nitro-blue-tetrazolium chloride (NBT) can be reduced into purple tetrazole-blue-diformazan in the presence of superoxide anion radical, the amount of generated superoxide anion radicals can be quantitatively detected by measuring the optical density (OD) of the reduced products at 560 nm [20]. The activity of the Au–Pt NCs for scavenging superoxide anion radicals can be determined by the calculating the difference of optical density compared with that of the control experiments. The typical processes for NBT-reduction assays were performed in the dark room. The reaction medium with a total volume of 3 mL, contained 0.05 M phosphate buffer, 0.013 M methionine, 0.1 μM EDTA, 2 μM riboflavin, 75 μM NBT and the as-prepared nanoparticles (0.12 nM) or SOD (~20 units/mL). The superoxide anion radicals were generated via ultraviolet irradiating with a 365-nm UV lamp. After an irradiation of 30 min, 3 mL DMSO was added to improve the solubility of tetrazole-blue-diformazan. Then the nanoparticles were removed by centrifugation and the optical density at 560 nm of supernatant solutions was measured with UV–visible spectrometer according to previous reports. Thus, the activity (f) of Au–Pt NCs for superoxide anion radicals scavenging can be determined according to the equation, $f = (OD_e - OD_c)/OD_c$, where the OD_e and OD_c are the optical density of experimental and control samples, respectively.

2.3.2. Hydrogen peroxide scavenging by fluorescent spectroscopy

The activity of Au–Pt NCs for scavenging H_2O_2 was tested with commercial carboxy-H2DCFDA dyes, which can quickly transform into fluorescent products in the presence of H_2O_2 or other reactive oxidative species. Firstly, the nanoparticles (with a final concentration of 0.12 nM) or catalase (100 units/mL) was mixed with H_2O_2 solution (1 mM in 0.1 M PBS) and incubated for 30 min at 25°. Then the nanorods were removed by centrifugation and the carboxy-H2DCFDA dyes were added into the supernatant solutions with a final concentration of 10 μM. After stirring for several minutes, the fluorescence spectrum of the mixture was recorded with fluorescence spectroscopy. Also, the activity of Au–Pt NCs for H_2O_2 scavenging can be determined by calculating the difference of fluorescence intensity between experimental and control samples.

2.4. Surface modification and characterization of functionalized Au–Pt NCs

Since the gold nanorods are generally synthesized in a solution with concentrated CTAB, which is reported to be a kind of highly toxic molecule to cells [21], removing the CTAB on the surface of gold nanorods is requisite for the application of biomedicine and bioengineering. Thus, the surface modification of the Au–Pt NCs was performed by mixing the thiolated cationic ligand at a final concentration of 5 μM, MUTAB with the purified Au–Pt NCs (~200 pM) for 2 h. Then the replaced CTAB molecules were removed by centrifugation and the precipitation was redispersed in water. The ligand exchange process was repeated for 3 times for a complete ligand exchange. After that, the Au–Pt NCs solution was mixed with 1 mL of 200 mg/L BSA solution for 1 h and the BSA molecules were absorbed onto the surface of MUTAB capped Au–Pt NCs via electrostatic interaction. The absorption spectrums and zeta potential of the Au–Pt NCs were measured to confirm the surface functionalization for each step.

2.5. Cell culture and cell imaging

HaCaT cell lines were purchased from American Type Culture Collection (ATCC, USA). The cells were maintained in DMEM (Dulbecco's modified Eagle's medium with high glucose, GIBCO) supplemented with 10% fatal bovine serum (GIBCO) and 1% penicillin/streptomycin (Invitrogen) at 37 °C, 5% CO_2 in a humidified atmosphere. For the experiments of cell imaging, the cells were cultured on a cleaned cover-glass in a plastic cell culture dish. Cellular uptake of nanoparticles was performed by adding 100 μL of Au–Pt NCs into the cell culture medium and incubating for 4 h and the residual Au–Pt NCs in the medium were removed by refreshing the culture medium. Then the cover-glass was inverted and placed on a glass slide with a concave cavity in the centre, to which the cell culture medium was applied to keep the cells alive during the observation under microscope. Because the scattering intensities of the nanoparticles are much higher than intracellular organelles, the amount of the particles uptake by the cells can be evaluated directly from the dark-field images. Cell viability after treated with the Au–Pt NCs was tested by using a standard MTT assay according to previous reports [22]. For the study of cellular oxidative stress, the carboxy-H2DCFDA dyes were added into cell culture medium at a final concentration of 10 μM and incubated for 15 min. The cells with and without treatment of 100 μM H_2O_2 were used as positive and negative controls, respectively. After irradiating with 365-nm UV light for 0, 30, 60 and 90 min, the induced cellular oxidative stress in the presence or absence of Au–Pt NCs were then detected with the commercial dyes, where the irradiation power of the UV lamp was 16 mW and the distance between the UV lamp and the cell culture dish was around 15 cm. Cell morphology changes after UV irradiation were directly analyzed via counting the cell areas variations in the dark-field images.

3. Results and discussion

3.1. Characterization of the active Au–Pt NCs

From the results of TEM characterization in Fig. 1A and B, we can see that there are lots of spiny Pt nanostructures on the

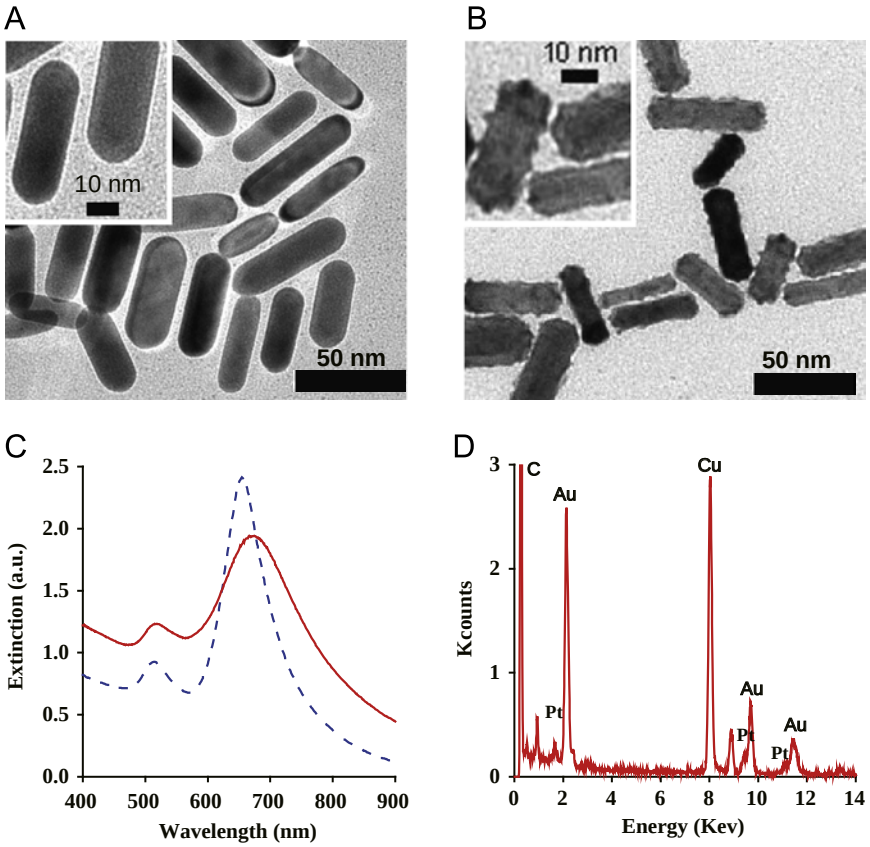

Fig. 1. Characterization of the prepared nanoparticles. (A) TEM images of GNRs, (B) TEM images of Au–Pt NCs, (C) UV-visible spectrum of GNRs (blue–dashed) and Au–PtNCs (red–solid), (D) EDX spectrum of the Au–Pt NCs.

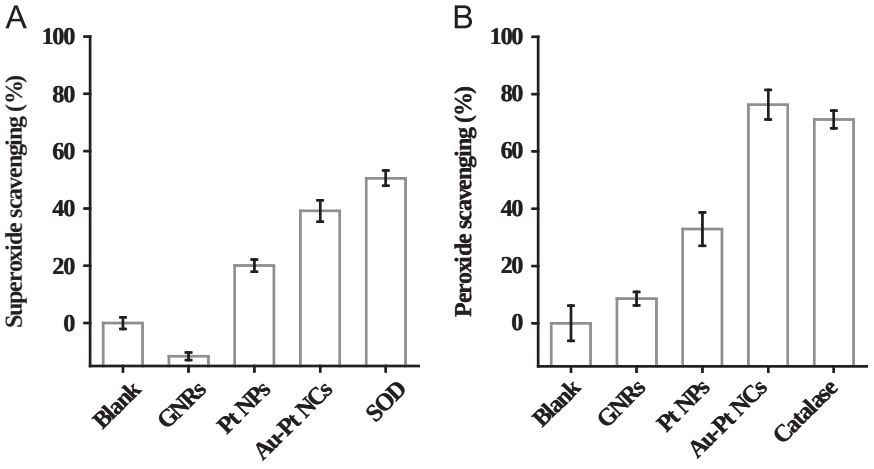

Fig. 2. SOD-like and peroxidase-like activity of Au–Pt NCs. Comparison of superoxide (A) and peroxide (B) scavenging activity. The concentrations of GNRs, Pt NPs and Au–Pt NCs are all 0.12 nM, and the concentrations of SOD and catalase are 20 units/mL and 100 units/mL.

smooth surface of GNRs, which make the Au–Pt NCs look like sea-cucumbers with highly rough surface. The remarkable red shift of plasmonic absorption peak (Fig. 1C) and the results of EDX spectroscopy (Fig. 1D) indicate the formation of Pt nanostructures on the surface of GNRs. Due to the high surface area of the spiny nanostructures and synergistic effect [23,24], the prepared Au–Pt NCs should possess a high catalytic activity in accelerating decomposition of reactive radicals and molecules.

In order to confirm this hypothesis, classical assays for catalyzing the dismutation of superoxide anion radicals and hydrogen peroxide were performed. Typical NBT-reduction assays, commonly used to determine the activity of SOD for eliminating superoxides, were applied for determining the superoxide scavenging activity of the prepared Au–Pt NCs and other materials including the natural SOD. As shown in Fig. 2A, the Au–Pt NCs were able to clear around 40% of the generated superoxides, which is a little lower than natural SOD (50%), but notably higher than GNRs and Pt nanoparticles alone. Next, we measured the peroxide scavenging activities of the Au–Pt NCs by determining the amount of residual hydrogen peroxide (H_2O_2) with fluorescence spectroscopy by using a commercial ROS-responsive carboxy-H2DCFDA dye as the probe. As shown in Fig. 2B, approximately 76% of H_2O_2 in the solution was decomposed by Au–Pt NCs, which is comparable to that by catalase (71%) and much larger than that by Pt nanoparticles and GNRs. These results

prove that the enzyme-mimic Au–Pt NCs are highly active in ROS scavenging compared with natural enzymes, suggesting their potential use for reducing cellular oxidative stress.

3.2. Surface functionalization of Au–Pt NCs

To obtain active nanoparticles with high cellular uptake efficiency and good biocompatibility, a layer-by-layer strategy was applied for the surface modification of Au–Pt NCs. Due to the strong bonding between thiols and gold [25], the residual cytotoxic CTAB surfactant on the surface of the Au–Pt NCs was replaced by using an alkyl cationic thiol, (11-mercaptoundecyl)-N,N,N-trimethylammonium bromide (MUTAB) through ligand exchange. Then, bovine serum albumin (BSA) was adsorbed onto the surface of Au–Pt NCs via electrostatic interaction for better biocompatibility [26]. UV–visible spectroscopy and zeta potential measurements were utilized for characterization of the surface-modification process (Table 1 and Fig. S1). After ligand exchange, a blue shift of the absorption maximum occurred, indicating the replacement of CTAB by MUTAB. Further adsorption of BSA molecules onto the surface of Au–Pt NCs induced a clear red shift of the absorption peak and the nanoparticles became negatively charged. Finally, the ROS-scavenging activity of the surface modified Au–Pt NCs was tested (Fig. S2), and the results indicated that the modified Au–Pt NCs are still highly active.

Table 1
Results of UV–visible spectroscopy and zeta potential measurements for the step-by-step surface modification.

	LSPR λ_{max} (nm)	Zeta potential (mV)
Au–Pt NCs	672	$+29.8 \pm 12.6$
MUTAB Au–Pt NCs	668	$+28 \pm 10.8$
BSA-MUTAB-Au–Pt NCs	675	-10.9 ± 4.8

3.3. Cellular cytotoxicity test of Au–Pt NCs

Because UV irradiation most likely induces cell damage in the outmost layer of the skin, we chose human keratinocyte cells (HaCaT cells) as the model system. After incubating HaCaT cells with the modified Au–Pt NCs for 4 h, as expected, there were lots of Au–Pt NCs dispersed in the cytoplasm even when the particle concentration added into cell culture medium was as low as 6 pM (Fig. 3A). Compared with the results from control experiments, the efficiency of cellular uptake was greatly improved by tuning the surface properties of the nanoparticles as mentioned above. Furthermore, after washing off excess nanoparticles on the cell surface and culturing the cells for 24 h with fresh medium, a higher portion of the internalized modified nanoparticles were retained by the cells than the particles without surface modification (Fig. S3). Then, typical MTT assays were performed to investigate the cellular cytotoxicity of the Au–Pt NCs. Our results indicated that the uptake of modified Au–Pt NCs did not induce obvious decrease of cell viability ($>80\%$ at each case) even at relative large particle concentrations, while the cell viability was remarkably reduced by unmodified Au–Pt NCs (Fig. 3B). Therefore, cellular uptake efficiency and biocompatibility of Au–Pt NCs can be greatly promoted by surface functionalization. To investigate the capability of the modified Au–Pt NCs against cellular oxidative stress after entering the cells, the intracellular ROS levels were determined by adding 10 μM carboxy-H2DCFDA dye into the

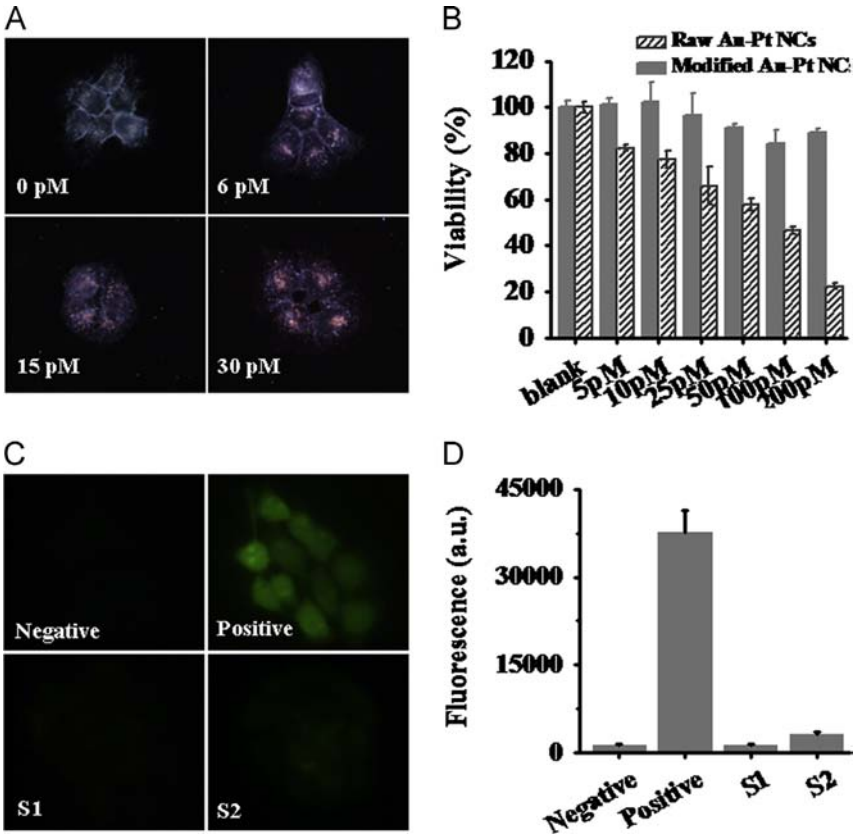

Fig. 3. Cellular uptake and cellular responses towards modified Au–Pt NCs. (A) Cellular uptake of the modified Au–Pt NCs as shown by dark-field microscopy. (B) Results of the MTT assays after incubating the cells with Au–Pt NCs for 48 h. (C) Fluorescence imaging of ROS levels in blank cells (negative) and cells treated with 100 μM H_2O_2 (positive), 30 pM Au–Pt NCs (S1), 30 pM Au–Pt NCs, and 100 μM H_2O_2 (S2), respectively. (D) Corresponding average fluorescence intensity per cell for the cases in (C).

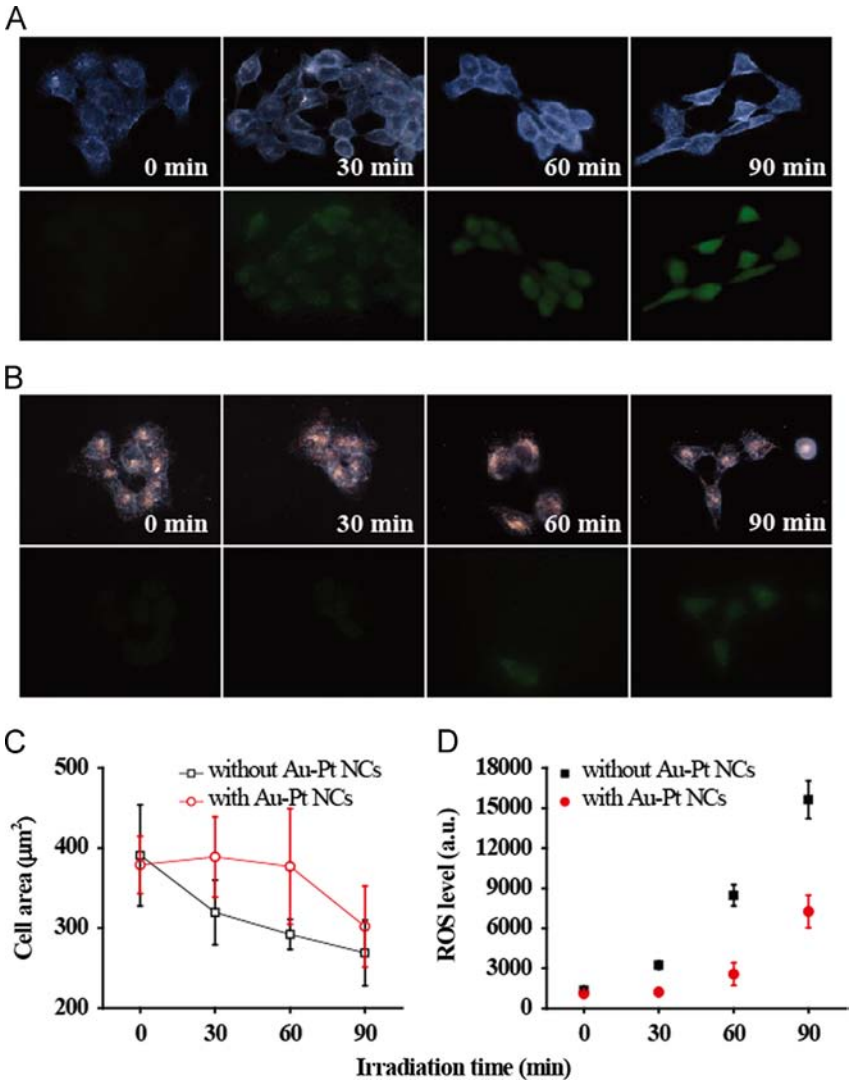

Fig. 4. Preventing UV induced cell damage with Au–Pt NCs. Dark-field (upper) and fluorescent (lower) images of cells after being irradiated with UV light for 0, 30, 60 and 90 min in the absence (A) or presence (B) of Au–Pt NCs. Also shown are corresponding cell morphology changes (C) and cellular ROS analysis (D) after UV irradiation.

culture medium [27]. Fig. 3C and D show the ROS levels in blank cells (negative control) and cells treated with 100 μM H_2O_2 (positive control), 30 pM Au–Pt NCs (S1) and 30 pM Au–Pt NCs and then 100 μM H_2O_2 (S2), respectively. It can be seen that with Au–Pt NCs inside the cells, there was no elevation of the ROS level, but the intracellular ROS level in the positive control was greatly enhanced compared with that of blank cells. The ROS stress in cells of group S2 is remarkably reduced by the Au–Pt NCs compared with positive control experiments, indicating that the surface modified Au–Pt NCs in skin cells are still very active and can be used to reduce cellular oxidative damage induced by H_2O_2 treatment.

3.4. *Preventing UV-induced cell damage with the active Au–Pt NCs*

To validate the application of these active Au–Pt NCs for protecting cells from UV induced oxidative damage by scavenging intracellular ROS *in vivo*, we incubated the Au–Pt NCs with human skin cells and then examined the ROS stress levels after UV irradiation with different time. After a 4 h incubation with cells, the residual nanoparticles were removed by refreshing the culture medium. The cells were irradiated with 365-nm UV light for 0 min, 30 min, 60 min and 90 min, respectively, with the distance between the handheld UV lamp and the cell culture surface at about 15 cm. The UV induced cell shrinkage was determined by calculating the changes of cell areas under dark-field microscopy and the cellular ROS levels were determined with carboxy-H2DCFDA dye under fluorescent microscopy. The cells irradiated with UV light without pretreatment of Au–Pt NCs were used as the control. As can be seen in Fig. 4A, the ROS levels and cell shrinkage due to subsequent oxidative damage can be much aggravated by prolonging the UV-irradiation time. However, UV induced ROS stress in the cells treated with Au–Pt NCs is markedly less than that in the control experiments for the same irradiation time, implying that the Au–Pt NCs can effectively scavenge cellular ROS produced by UV light in living cells (Fig. 4B). Until the cells were exposed to UV light longer than 60 min, the cell shrinkage and the elevation of cellular ROS become observable even with the protection of Au–Pt NCs (Fig. 4C and D). That is, the effective time for protecting from UV induced cell damage with the prepared NMs is around 60 min. It is reasonable because UV rays with high energy can directly deteriorate cellular biomolecules such as proteins and DNA during long-time UV irradiation.

Furthermore, we examined the influence of UV irradiation on cell proliferation with or without the Au–Pt NCs. Owning to the checkpoints and repairing mechanisms in cell cycle, there is a delay of proliferation for cells suffering from oxidative damage [28,29]. Fig. 5 shows that there was an obvious difference in proliferation rates of the cells after they were irradiated for 60 min

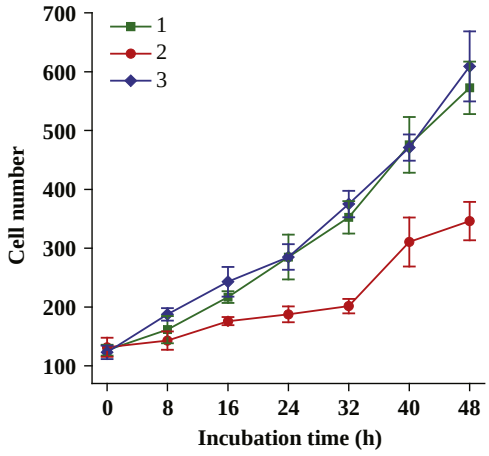

Fig. 5. Cell proliferation after irradiating for 0 min (1), and 60 min without (2) or with (3) the protection of Au–Pt NCs.

with vs. without the pretreatment of Au–Pt NCs. It can be seen that the proliferation rate of the cells with the protection of Au–Pt NCs was almost the same as that of the cells without UV irradiations. But for cells without the protection of Au–Pt NCs, there was an apparent delay in cell proliferation. These results suggested that UV induced cellular damage through the indirect route of ROS interaction can be effectively prevented with the prepared Au–Pt NCs in our study. Thus, these biocompatible and active Au–Pt NCs can be applied to scavenge UV generated cellular ROS in real time and prevent subsequent cellular oxidative damage to the cells.

4. Conclusions

In this study, we have prepared a new type of enzyme-mimic Au–Pt NCs that can directly catalyze the decomposition of reactive oxygen species. The surface modified Au–Pt NCs exhibited high cellular uptake efficiency and excellent biocompatibility in human skin cells. Moreover, the active Au–Pt NCs were capable of scavenging UV induced cellular ROS and preventing subsequent oxidative damage to the cells *in vivo*. These results suggest that the Au–Pt NCs can be potentially used for the prevention and therapy of ROS-mediated diseases.

Acknowledgments

The authors are grateful for the financial support by NSFC 21127009, NSFC 91027037 and Hunan University 985 Fund.

Appendix A. Supplementary material

Supplementary data associated with this article can be found in the online version at http://dx.doi.org/10.1016/j.talanta.2013.12.020.

References

[1] F. Suzuki, A. Han, G.R. Lankas, H. Utsumi, M.M. Elkind, Cancer Res. 41 (1981) 4916.
[2] J. Dove, Environ. Edu. Res. 2 (1996) 89.
[3] I.E. Kochevar, J. Invest. Dermatol. 77 (1981) 59.
[4] D. Kulms, E. Zeise, B. Poeppelmann, T. Schwarz, Oncogene 21 (2002) 5844.
[5] B.P. Yu, Physiol. Rev. 74 (1994) 139.
[6] W. Davis, Z.e. Ronai, K.D. Tew, J. Pharmacol. Exp. Ther. 296 (2001) 1.
[7] D.E. Heck, A.M. Vetrano, T.M. Mariano, J.D. Laskin, J. Biol. Chem. 278 (2003) 22432.
[8] J.J. Yin, F. Lao, P.P. Fu, W.G. Wamer, Y. Zhao, P.C. Wang, Y. Qiu, B. Sun, G. Xing, J. Dong, X.J. Liang, C. Chen, Biomaterials 30 (2009) 611.
[9] L. Zhang, L. Laug, W. Münchgesang, E. Pippel, U. Gösele, M. Brandsch, M. Knez, Nano Lett. 10 (2009) 219.
[10] Z. Chen, J.J. Yin, Y.T. Zhou, Y. Zhang, L. Song, M. Song, S. Hu, N. Gu, ACS Nano 6 (2012) 4001.
[11] X. Liu, W. Wei, Q. Yuan, X. Zhang, N. Li, Y. Du, G. Ma, C. Yan, D. Ma, Chem. Commun. 48 (2012) 3155.
[12] N.H. Alsharif, C.E.M. Berger, S.S. Varanasi, Y. Chao, B.R. Horrocks, H.K. Datta, Small 5 (2009) 221.
[13] M. Kajita, K. Hikosaka, M. Iitsuka, A. Kanayama, N. Toshima, Y. Miyamoto, Free Radical Res. 41 (2007) 615.
[14] J. Fan, J.J. Yin, B. Ning, X. Wu, Y. Hu, M. Ferrari, G.J. Anderson, J. Wei, Y. Zhao, G. Nie, Biomaterials 32 (2011) 1611.
[15] W. He, Y. Liu, J. Yuan, J.J. Yin, X. Wu, X. Hu, K. Zhang, J. Liu, C. Chen, Y. Ji, Y. Guo, Biomaterials 32 (2011) 1139.
[16] M. Ma, Y. Zhang, N. Gu, Colloid Surf. A: Physicochem. Eng. Asp. 373 (2011) 6.
[17] B. Xiong, J. Cheng, Y. Qiao, R. Zhou, Y. He, E.S. Yeung, J. Chromatogr. A 1218 (2011) 3823.
[18] M. Grzelczak, J. Pérezjuste, F.J. García de Abajo, L.M. Liz Marzán, J. Phys. Chem. C 111 (2007) 6183.
[19] Y. Mei, G. Sharma, Y. Lu, M. Ballauff, M. Drechsler, T. Irrgang, R. Kempe, Langmuir 21 (2005) 12229.
[20] Y. Sun, L.W. Oberley, Y. Li, Clin. Chem. 34 (1988) 497.
[21] E.E. Connor, J. Mwamuka, A. Gole, C.J. Murphy, M.D. Wyatt, Small 1 (2005) 325.
[22] D. Gerlier, N. Thomasset, J. Immunol. Methods 94 (1986) 57.
[23] M. Arenz, K.J.J. Mayrhofer, V. Stamenkovic, B.B. Blizanac, T. Tomoyuki, P.N. Ross, N.M. Markovic, J. Am. Chem. Soc. 127 (2005) 6819.
[24] D. Mott, J. Luo, P.N. Njoki, Y. Lin, L. Wang, C.J. Zhong, Catal. Today 122 (2007) 378.
[25] L. Vigderman, P. Manna, E.R. Zubarev, Angew. Chem. Int. Ed. 124 (2012) 660.
[26] A.M. Alkilany, P.K. Nagaria, C.R. Hexel, T.J. Shaw, C.J. Murphy, M.D. Wyatt, Small 5 (2009) 701.
[27] Y. Pang, L. Campbell, B. Zheng, L. Fan, Z. Cai, P. Rhodes, Neuroscience 166 (2010) 464.
[28] A. Hirao, Y.Y. Kong, S. Matsuoka, A. Wakeham, J. Ruland, H. Yoshida, D. Liu, S.J. Elledge, T.W. Mak, Science 287 (2000) 1824.
[29] A. Sancar, L.A. Lindsey-Boltz, K. ÜnsalKaçmaz, S. Linn, Annu. Rev. Biochem. 73 (2004) 39.